BJ www.biochemj.org

BJ ChemBio

Biochem. J. (2012) **443**, 549–559 (Printed in Great Britain) doi:10.1042/BJ20111779

online data

First identification of small-molecule inhibitors of Pontin by combining virtual screening and enzymatic assay

Judith ELKAIM*, Michel CASTROVIEJO†, Driss BENNANI*, Said TAOUJI‡, Nathalie ALLAIN‡, Michel LAGUERRE*, Jean ROSENBAUM‡, Jean DESSOLIN*[1] and Patrick LESTIENNE‡[1]

*Molecular Modeling Group, IECB-CNRS-Université de Bordeaux, UMR 5248, 2 rue R. Escarpit, F-33607 Pessac, France, †Platform Protein Expression and Purification, CNRS, UMR 5234, 146 rue L. Saignat, F-33076 Bordeaux Cedex, France, and ‡Physiopathologie du Cancer du Foie, INSERM U1053-Université de Bordeaux, 146 rue L. Saignat, F-33076 Bordeaux Cedex, France

The human protein Pontin, which belongs to the AAA+ (ATPases associated with various cellular activities) family, is overexpressed in several cancers and its silencing *in vitro* leads to tumour cell growth arrest and apoptosis, making it a good target for cancer therapy. In particular, high levels of expression were found in hepatic tumours for which the therapeutic arsenal is rather limited. The three-dimensional structure of Pontin has been resolved previously, revealing a hexameric assembly with one ADP molecule co-crystallized in each subunit. Using Vina, DrugScore and Xscore, structure-based virtual screening of 2200 commercial molecules was conducted into the ATP-binding site formed by a dimer of Pontin in order to prioritize the best candidates. Complementary to the *in silico* screening, a versatile and sensitive colorimetric assay was set up to measure the disruption of the ATPase activity of Pontin. This assay allowed the determination of inhibition curves for more than 20 top-scoring compounds, resulting in the identification of four ligands presenting an inhibition constant in the micromolar concentration range. Three of them inhibited tumour cell proliferation. The association of virtual screening and experimental assay thus proved successful for the discovery of the first small-molecule inhibitors of Pontin.

Key words: ATPase activity, enzymatic assay, Pontin, small-molecule inhibitor, TATA-box-interacting protein 49 (TIP49), Vina, virtual screening.

INTRODUCTION

Pontin, also known as TIP (TATA-box-binding protein) 49 or RUVBL (RuvB-like) 1, and its homologue Reptin (TIP48, RUVBL2), with which it shares 40 % sequence identity and 65 % homology [1], belong to the AAA+ (ATPase associated with various cellular activities) family and display homologies with the bacterial RuvB helicase [2]. The structure of Pontin shows characteristic ATPase Walker A and B domains; the Walker A motif plays a role in nucleotide binding and in metal-ion co-ordination, whereas the Walker B domain contains residues involved in metal-ion co-ordination and ATP hydrolysis. Additional domains such as the sensors 1 and 2, and the arginine finger (Arg^{357}) interact with the γ-phosphate and play an important role in intersubunit communication and interactions [3]. The arrangement in hexameric complexes, shared with other AAA+ family members [4], was deduced from X-ray diffraction analysis and from electron microscopy experiments either for Pontin alone or in complex with Reptin in yeast and human [5–7]. The three-dimensional reconstitution of electron microscopy images revealed a dodecameric edifice with a central cavity forming a tunnel compatible with the diameter of potential polynucleotides. As confirmed by the crystallographic structure of Pontin alone published by Matias et al. in 2006 [3], this complex was supposed to be composed of a homohexamer of Pontin superimposed on top of a homohexamer of Reptin, for which no three-dimensional structure existed. However, another structure has been recently described by the same team, displaying important differences with the original one, mainly in the hexameric arrangements which are not composed of Pontin alone [8]. (This article presenting a new structure for the hexameric assembly was released online after the present paper had been submitted for review. It was therefore not taken into account in our simulations.) In fact, the proposed structure presents a heterohexamer composed of alternating subunits of Pontin and Reptin which will probably have a great significance in the mechanistic comprehension of this complex.

Most publications agree that human Pontin and Reptin are indeed endowed with an ATPase activity either alone, or in heteromeric complexes [9]. Pontin and Reptin belong to several multi-protein complexes in the nucleus [10], where they are thought to participate in chromatin remodelling [11,12], double-strand break DNA repair [13] and regulation of transcription [14]. They notably interact with the oncogenic transcription factors β-catenin and c-Myc and modulate their activities [15,16]. They are also involved in the biogenesis and assembly of ribonucleoprotein complexes such as snoRNPs (small nucleolar ribonucleoproteins) [17,18] and telomerase [19].

We have reported previously that both Pontin [20] and Reptin [21] were overexpressed in human hepatocellular carcinoma. Overexpression of these proteins was also found in a number of other human cancers [9]. *In vitro* silencing of either Pontin or Reptin led to tumour cell growth reduction [20,21]. Furthermore, *in vivo* silencing of Reptin in xenografted tumours dramatically reduced tumour progression [22]. These features indicate that Pontin and Reptin could be good candidates for cancer therapy.

With the use of Walker A or B mutants of Pontin devoid of ATPase activity, several authors have suggested that the ATPase activity of Pontin is required for growth and viability in yeast cells [1,23,24]. The same method allowed the demonstration that the D302N Walker B mutant of Pontin did not support telomerase

Abbreviations used: AAA+, ATPase associated with various cellular activities; MTS, 3-(4,5-dimethylthiazol-2-yl)-5-(3-carboxymethoxyphenyl)-2-(4-sulfophenyl)-2*H*-tetrazolium; PTP1B, protein tyrosine phosphatase 1B; RUVBL, RuvB-like; TIP, TATA-box-binding protein.

[1] Correspondence may be addressed to either of these authors (email j.dessolin@iecb.u-bordeaux.fr for molecular modelling aspects or patrick.lestienne@inserm.fr for biochemical aspects).

biogenesis in human cells [19] and inhibited cell transformation by several oncogenes such as c-Myc [16], β-catenin [25] or E1A [26]. Therefore targeting the ATPase activity of Pontin appears to be a suitable strategy against cancer.

In the present study, we present two complementary approaches for the discovery of inhibitors of Pontin. No report of small-molecule inhibitors for Pontin or Reptin has been made to date, since a major drawback encountered by several teams in the design of an enzymatic assay for Pontin was the low activity of the protein, if any, when detected by the hydrolysis of radiolabelled ATP, yielding ADP and P_i [3,6,27–29]. On top of that, this method is time-consuming owing to the use of TLC, presents difficulties because of the short half-life of ^{32}P, and is slightly harmful and difficult to handle in a standard laboratory. An easy-to-handle colorimetric assay that only requires a spectrophotometer was designed in order to overcome these limitations and allowed the identification of 29 inactive compounds from the French Chimiothèque Nationale. These molecules presented no inhibitory effect on the ATP hydrolysis displayed by Pontin.

In order to select potential inhibitors, we took advantage of the three-dimensional structure of the hexameric complex of Pontin with bound ADP, which has been resolved by X-ray crystallography [3], to provide a model for structure-based virtual screening of commercial chemical compounds in the ATPase catalytic centre of Pontin. The main criterion for the database selection was that the molecules were to be available for experimental testing, which is why two commercial databases of ligands were used in the virtual screening: the Calbiochem database of Inhibitors® from Merck and the Prestwick Chemical Library®. Another advantage was that all of the molecules from these databases display a known activity and are biologically relevant or 'drug-like', plus their ADME-Tox (absorption, distribution, metabolism, excretion and toxicology) data are documented. The dockings were conducted with Vina [30], then the compounds were rescored with DrugScore [31,32] and Xscore [33], and the top-scoring ligands were selected via consensus scoring.

Finally, priority compounds identified via virtual screening *in silico* were tested in the enzymatic assay *in vitro* for their activity against the ATPase activity of human recombinant Pontin, then in cultured tumour cells for their anti-proliferative effect.

EXPERIMENTAL

Materials

HPLC-purified oligonucleotides were from Eurogentech. Selected molecules were from Merck Bioscience and Prestwick. Protease inhibitor tablets were from Roche. The pET21-N-ter-His_6-TIP49 plasmid was a gift from Dr I.R. Tsaneva (Structural and Molecular Biology Group, University College London, London, U.K.). Superdex G 200 HR column was from GE Healthcare. Ni-NTA (Ni^{2+}-nitrilotriacetate) superflow cartridge was from Qiagen. Rottlerin, PTP1B (protein tyrosine phosphatase 1B) inhibitor {3-(3,5-dibromo-4-hydroxy-benzoyl)-2-ethyl-benzofuran-6-sulfonicacid-[4-(thiazol-2-ylsulfamyl)-phenyl]-amide} and Akt1/2 inhibitor {1,3-dihydro-1-[1-({4-(6-phenyl-1*H*-imidazo[4,5-*g*]quinoxalin-7-yl)phenyl}methyl)-4-piperidinyl]-2*H*-benzimidazol-2-one} were from Calbiochem. Pranlukast {N-[4-oxo-2-(1*H*-tetrazol-5-yl)-4*H*-chromen-7-yl]-4-(4-phenylbutoxy)benzamide} was from Prestwick. Imidazole buffer solution and other reagents were from Sigma.

The oligonucleotides used in the present study were (underlined bases are complementary): single strand (43-mer), 5′-GCTCGCTACCCGGGGATCCTCTAGAGTCATCAGTGCAAGACCG-3′, hairpin (44-mer), 5′-TCGCTCTTCTACTATGAACCCCCCTCCCCATTTTTGGGGAGGGG-3′, and double-stranded (64-mer), 5′-TCGCTCTTCTACTATGAACCCCCCTCCCCATTTTTGGGGAGGGGGGTTCATAGTAGAAGAGCGA-3′.

Receptor preparation for docking

The crystal structure of Pontin bound with ADP (PDB code 2C9O) was used for docking [3]. Except for two loops from residues 142–155 and 248–276, the structure was complete. Those loops were far enough from the region of interest and therefore were not reconstructed before calculations. The structure was visualized using Discovery Studio 2.1 (Accelrys). All water molecules were removed and missing hydrogen atoms were added using Charmm forcefield. A minimization of the structure was conducted in the presence of bound ADP, using a Steepest Descent algorithm, 2000 steps with a 0.01 gradient, keeping the backbone of the protein fixed. The ADP-binding site is located at the interface between two subunits, therefore the docking was conducted on a dimer of Pontin to take into account potential interactions with the second subunit.

Ligand preparation for docking

The chosen commercial chemical databases are a collection of compounds selected for their high chemical and pharmacological diversity, as well as their documented bioavailability and safety in humans (according to the manufacturer). The mean Tanimoto coefficients are 0.1839 and 0.1265 respectively for Calbiochem and Prestwick, which mean a high structural diversity (calculated with OpenBabel 2.2.99 and FP2 from Daylight) [34].

Compounds from the Calbiochem Database of Kinase Inhibitors® were obtained in SD (structure file) format from the Merck Chemicals website (catalogue numbers are 539743, 539744, 539745 and 539746). The three-dimensional structures in MOL2 format were generated automatically using Catalyst in Discovery Studio via the *Prepare Ligands* protocol. All parameters were turned to False, except for Change Ionization, the maximum pH was set to 8.5 and the minimum to 6.5 in order to generate different protonation states. The structures obtained were then filtered with DBfilter 2.2.8 (a drug-like analyser for chemical library, distributed by the author S.-H. Wang, 2005). Molecules with a molecular mass lower than 200 Da or higher than 800 Da were rejected, as well as molecules with more than ten rotatable bonds. Only standard atoms such as hydrogen, carbon, nitrogen, oxygen, fluorine, chlorine, bromine, iodine, phosphorus or sulfur were allowed. All compounds in MOL2 format were translated into PDBQT files suitable for docking with the script *prepare_ligand4.py* from MGLTools 1.5.4 [35].

The same treatment was applied to the compounds from the Prestwick Chemical Library® (http://www.prestwickchemical.com/index.php?pa=26) available on request in SD format. The structures and PDBQT files were automatically generated using Discovery Studio and the *prepare_ligand4.py* script.

A total of 29 compounds from the French Chimiothèque Nationale were visually selected for experimental evaluation of their inhibition potential of Pontin ATPase. Because of a non-disclosure agreement, we cannot display these structures, but the identifications are available from J.D. upon request. These molecules were manually constructed in Discovery Studio, and *Dreiding Minimize* was used to reach a low-energy conformation. As described for the compounds from Calbiochem, the PDBQT input files were automatically prepared with the *prepare_ligand4.py* script. These compounds were incorporated into the Calbiochem database and used to evaluate the scoring functions on their ability to discriminate decoys from potential actives.

Charges automatically assigned to the ligands during the *Prepare Ligands* protocol are not equivalent to the ones assigned via *Dreiding Minimize*, but these charges are irrelevant, since Vina and all the scoring functions used in the present study recalculate their own partial charges for the ligands during calculation.

Docking and scoring

Autodock Vina 1.0.2 [30] was used for all dockings in the present study. Vina was derived from Autodock, but it achieves improvements in speed and accuracy over the latest release of Autodock (Autodock4 [36]). Besides, Vina calculations are run directly from the command line and automatically take advantage of multiple cores [37]. The ligands were docked using Vina, and then rescored using the stand-alone programs DrugScore and Xscore. For each ligand in the database, five docking experiments were conducted, each of them generating up to nine poses. The results from the five experiments were averaged, and the compounds were then ranked on the basis of their average scores for each individual scoring function or sorted via consensus scoring.

Rigid dimer

The ligands were considered flexible while the protein was held rigid. The docking grid was designed in order to include the whole cavity surrounding ADP in the crystallographic structure plus a margin of at least 3 Å (1 Å = 0.1 nm) in all directions. The resulting dimensions of the box were 20 Å×22 Å×20 Å. A total of 74 amino acids belonging to the first subunit and six amino acids belonging to the second subunit are fully or partially located inside the box. The parameters were kept at their default value. Each docking was conducted five times with five fixed seed numbers that were used for all ligands. The scores obtained for each function are the averages of these five experiments.

Flexible dimer

The system and parameters were similar to the rigid dimer, except that 11 torsions from four different residues were considered rotatable during docking.

Blind docking

The blind docking was conducted on a monomer of Pontin. The parameters were kept at their default values once again, but the search space was extended considerably to encompass the whole protein. The box dimensions were 58 Å×76 Å×70 Å.

The docking output PDBQT-formatted files were translated into PDB with in-house scripts and non-polar hydrogens were added in MOL2 format with OpenBabel 2.2.3 [38]. All poses generated by Vina were rescored using scoring functions from DrugScore and Xscore, resulting in ten different scores for each pose.

The *Consensus scoring* protocol from Discovery Studio was used to create a list of priority compounds.

Post-experimental check

Manual checking of the three-dimensional structures of the ligands was performed on the top-scoring molecules only, after calculations. The automatic generation of the structures had eventually produced some errors, mostly on heterocyclic aromatic features. Therefore all molecules included in the best consensus for both databases were checked visually for errors, corrected and redocked if needed before the identification of compounds selected for experimental screening.

Enzyme purification

Human recombinant Pontin was purified from 2 litres of *Escherichia coli* BL21 culture essentially as described in [6] in 1–2 working days, with a two-step chromatographic procedure. Briefly, following 3 h of induction at 20 °C with 1 mM IPTG (isopropyl β-D-thiogalactopyranoside), cells were lysed in 40 ml of buffer A containing 20 mM Tris/HCl (pH 7.5), 300 mM NaCl, 10 % (v/v) glycerol, 1 mM PMSF, 1 mM 2-mercaptoethanol, protease inhibitor tablet, 0.5 % Nonidet P40 and 20 mg/ml lysozyme. Upon incubation for 15 min, the lysate was sonicated extensively and cleared by centrifugation at 45 000 ***g*** for 15 min. The supernatant was loaded on to a 5 ml Ni-NTA Superflow cartridge column and washed with buffer B containing 20 mM Tris/HCl (pH 7.5), 20 mM imidazole, 300 mM NaCl, 10 % (v/v) glycerol and 1 mM 2-mercaptoethanol. The eluted fractions collected upon a 250 mM step with buffer B containing 500 mM imidazole were then purified on to a Superdex G200 (1 cm×30 cm) in buffer C (buffer B without imidazole). Fractions were analysed by SDS/PAGE (12 % gels), pooled and dialysed overnight in buffer C containing 50 % glycerol, then stored at − 80 °C.

Enzymatic assays

The hydrolysis of ATP into ADP and P_i was measured by the change in absorbance of the dye Malachite Green in the presence of phosphomolybdate complexes using the PiColorLock Gold assay from Gentaur.

The enzymatic reactions were performed in a final volume of 100 μl at 37 °C. The assay contained a final concentration of 20 mM Tris/acetate buffer (pH 7.5), 10 mM magnesium acetate, 0.5 mM 2-mercaptoethanol, 100 pmol of DNA, 10 % (v/v) DMSO and catalytic amounts of Pontin. Various serial dilutions of inhibitors dissolved in DMSO were added to a final volume of 80 μl. The reactions were started by the addition of 20 μl of the required final concentration of ATP, and its hydrolysis into ADP and P_i was detected by the colorimetric assay. The reaction rates were measured by taking 20 μl aliquots at several times and distributed into 96-well plates each containing 20 μl of Picolor Gold and 60 μl of water for at least 10 min at room temperature (22 °C). The stain was then stabilized with 10 μl of 'Stabilizer' for 30 min at room temperature. The A_{620} was measured using a spectrophotometer (Labsystems Multiskan Bichromatic) and correlated against a standard curve of P_i. The slopes were determined, thus providing the reaction rates. All experiments were carried out in triplicate.

The reproducibility of the assay was tested by measuring the *Z*' value. This was done by measuring the reaction rates over 30 min with 10 μM Pontin and 1 mM ATP. The *Z*' value was deduced from 48 reaction rates and found to be equal to 0.7. This value indicates the good reproducibility of the assay since accepted values of *Z*' lie between 0.5 and 1 [39].

Inhibition studies

Molecules were dissolved in DMSO. The final amount of DMSO was 10 % in the assays and we checked that it did not interfere with the reaction rates. We also checked that at the highest tested concentration of 50 μM, none of the molecules interfered with the assay in the presence of P_i (results not shown). For each concentration of inhibitor, the reaction rates were measured upon addition of 50 μM ATP. The IC_{50} (half maximal inhibitory concentration) was determined from two enzyme purifications. The reported IC_{50} values are the means for three independent experiments.

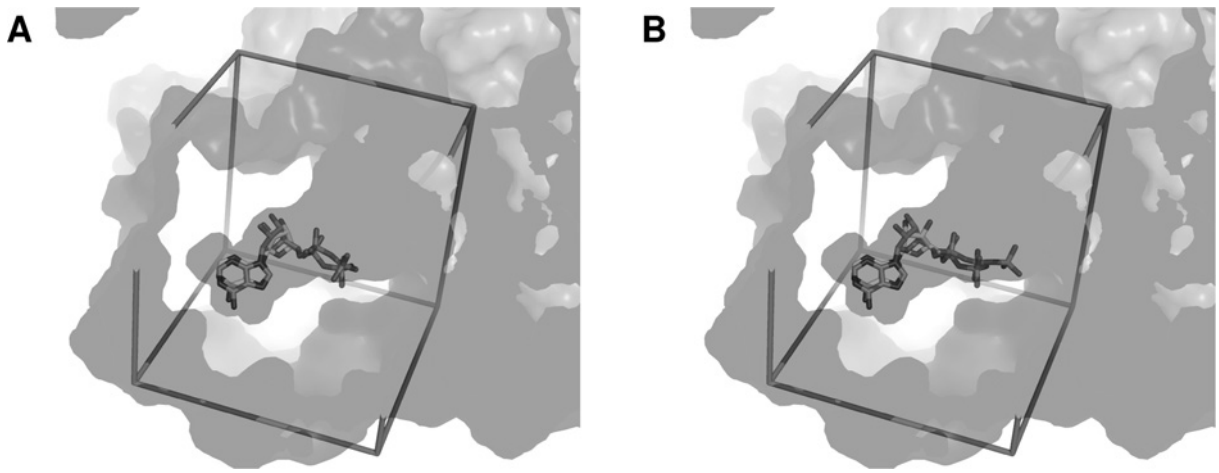

Figure 1 Docking of ADP and ATP

(**A**) Superimposition of crystallized ADP from PDB code 2C9O and docked ADP into the dimer of Pontin. The active site is represented as transparency, the search space box is represented as sticks. (**B**) Similar representation with docked ATP.

Cell proliferation experiments

The human hepatic tumour cell lines HuH7 and Hep3B were used. Cells were seeded at an initial density of 2500 cells/well in 96-well plates in DMEM (Dulbecco's modified Eagle's medium) with 10 % (v/v) fetal bovine serum. On the following day, they were treated with dilutions of test molecules in DMSO. The DMSO concentration was adjusted to 1 % in every well. After 4 days, cell numbers were estimated colorimetrically at 492 nm with the Cell-Titer 96 Aqueous One Solution Cell Proliferation Assay {MTS [3-(4,5-dimethylthiazol-2-yl)-5-(3-carboxymethoxyphenyl)-2-(4-sulfophenyl)-2*H*-tetrazolium] assay} from Promega. The growth index was calculated using eqn (1):

$$\text{Growth index} = \frac{D4_{\text{T}} - D0}{D4_{\text{DMSO}} - D0} \quad (1)$$

where $D4_{\text{T}}$ refers to the D_{492} with the test molecule at day 4, $D0$ is the D at day 0, and $D4_{\text{DMSO}}$ is the D at day 4 with DMSO alone.

RESULTS AND DISCUSSION

Docking strategy

As mentioned above, no Pontin inhibitor had ever been reported in the literature, but according to the enzymatic assay described below, an initial test on analogues of ATP had allowed us to identify 29 inactive compounds (results not shown). The ability to discriminate these decoys presented by our scoring functions either independently or in conjunction was used as a tool in order to evaluate the correctness of our results. At first, 900 compounds from the Calbiochem database plus the 29 decoys from the French Chimiothèque Nationale were used as a training set. Then, 1299 compounds from Prestwick were screened with regard to the results obtained with the Calbiochem training set.

Before the docking of the databases, ATP and ADP were docked into the active site to evaluate the quality of the model. The resulting poses were very similar to crystallized ADP (Figure 1). In particular, the adenine groups and the ribose of both molecules were superimposed on that of crystallized ADP, whereas only the highly flexible phosphate chain of ATP was notably displaced in some of the poses. At least 15 residues were involved in hydrophobic contacts with both ADP and ATP. In addition, the phosphate chain of ADP was stabilized by a network of eight hydrogen bonds coming from six different residues, whereas that of ATP could create up to 13 hydrogen bonds with eight residues, including five out of the six found in the case of ADP.

Constitution of priority lists of compounds by consensus scoring

Considering the very few experimental results, the approach based on individual scoring function was very likely to produce a large number of misranks. In this context, a consensus scoring strategy seemed a reasonable choice that could result in a reduction in the number of false negatives when selecting a limited number of molecules for experimental testing [40,41].

When considered individually, scoring functions from DrugScore$^{\text{CSD}}$ completely failed to eliminate the decoys from the top scorers, whereas Vina, DrugScore$^{\text{PDB}}$ and Xscore provided far better results. In conjunction with this, a very good consensus was obtained with HPscore from Xscore and SURF from DrugScore, which provided a large number of common top-scoring compounds including only one decoy, and adding Vina into the consensus allowed us to eliminate the last decoy in the top list. This improvement was followed by a significant decrease in the number of compounds in the intersection, but considering that the dockings were made with Vina and that its scoring function was used to generate the poses of the ligands, we decided that the Vina scoring function should be included in the consensus (see the Supplementary Online Data at http://www.BiochemJ.org/bj/443/bj4430549add.htm for a detailed description of the virtual screening results).

The consensuses carried out with these three independent scoring functions on the Calbiochem database led to the identification of 22 priority compounds ranking in the top 15 % for the three functions. Ten of them, i.e. approximately 1 % of the complete database, were randomly selected for experimental screening. The same procedure was applied to the 1299 compounds from the Prestwick Chemical Library®, leading to the prioritization of 23 new molecules and approximately the same percentage, namely 15 compounds, were chosen for testing.

Design of a versatile ATPase assay to measure Pontin activity

Human recombinant Pontin was purified via chromatography and the fractions eluted yielded various amounts of dodecameric,

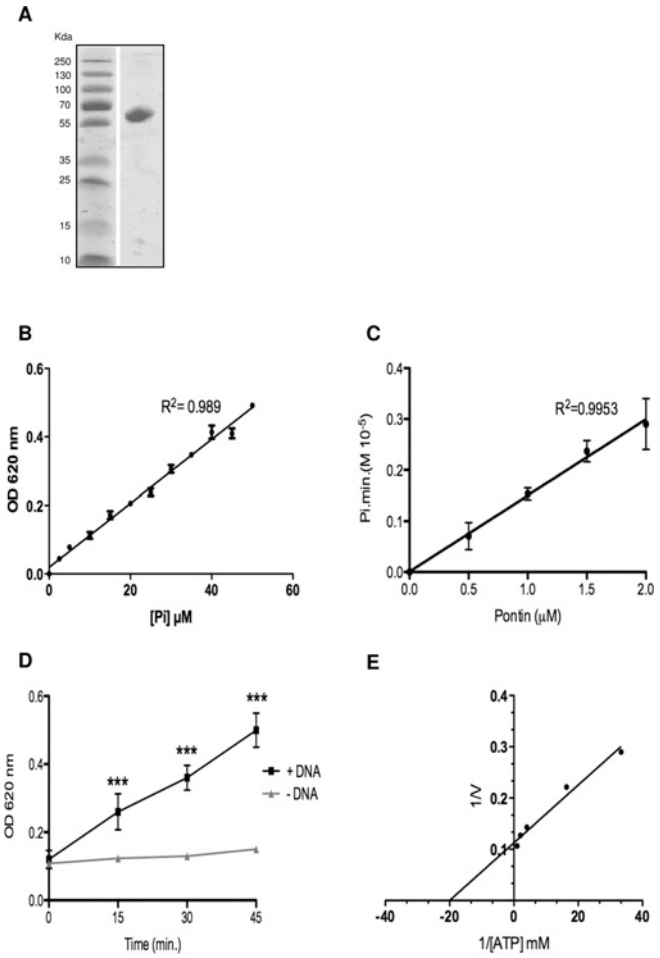

Figure 2 Enzymatic assays of Pontin ATPase activity

(**A**) SDS/PAGE of 5 μg of the monomeric Pontin fraction purified by chromatography on Superdex G200, and stained with Coomassie Brilliant Blue. Molecular masses are indicated in kDa. (**B**) Relationship between Pi concentration and A_{620} ('OD 620 nm'). Increasing concentrations of P_i were used with the Malachite Green assay, as described in the Experimental section. (**C**) Reaction rates according to the concentration of Pontin. The reported rates were determined for each concentration of Pontin during a 40 min incubation at 37 °C. Aliquots of 20 μl were taken every 10 min and the release of P_i was measured as in (**B**). (**D**) Effect of 10 μM DNA (43-mer) on the reaction rates in the presence of 2.5 μM Pontin and 2 mM ATP. The presence of DNA significantly increased the reaction rate (ANOVA, $P < 0.001$). Similar results were found with the other oligonucleotides described in the Experimental section. (**E**) Lineweaver–Burk representation of the reaction rates according to the ATP concentration in the assays. The concentration of Pontin was 2 μM. Results in (**B**)–(**D**) are means $\pm$ S.D. for three experiments.

hexameric and monomeric forms of Pontin as shown by elution volume and SDS/PAGE. When tested by the ATPase assay described below, only the purified monomeric fraction (Figure 2A) proved to be active, therefore all enzymatic experiments were conducted on the monomeric fraction.

A Malachite Green-derived assay that quantifies the green complex formed between Malachite Green, molybdate and free P_i was used to measure the enzyme activity in 96-well plates. As shown on Figure 2(B), A_{620} was proportional to the P_i concentration. The reaction rates were proportional to the enzyme concentration, and did not display apparent co-operativity (Figure 2C).

Almost no variation in the reaction rate of the ATPase catalysis could be detected in assays performed in the absence of oligonucleotides. In contrast, upon addition of an excess of single- or double-stranded DNA ([DNA]/[E] = 1–10), a 3-fold stimulation of the reaction rate was observed as shown in Figure 2(D) ($P < 0.01$). The effects of a single-stranded DNA of 43-mer, a hairpin of 44-mer and a perfect duplex DNA of 64-mer were studied. No significant differences were found whichever polynucleotide was used (results not shown). The ATP-hydrolysis reaction rate stimulation in the presence of DNA correlates with the presence of a polynucleotide-binding site detected by gel-shift assays with Pontin [3]. This activation by DNA is controversial in the literature, since it has been reported by many groups [1,42–44], but could not be detected by others [3,6,7]. However, the presence of DNA was essential in our assay to detect a sufficient activity in order to measure the IC_{50} of the ligands.

In order to test for potential inhibitors, the ATP concentration corresponding to the initial velocity was determined. Catalysis followed an asymptotic curve, allowing the determination of the K_m (Michaelis constant) with the Michaelis–Menten equation (eqn 2):

$$V = \frac{V_{max}[S]}{K_m + [S]} \quad (2)$$

Using the double-reciprocal plot described by Lineweaver–Burk, the K_m was found to be equal to 50 μM ($\pm$ 15 μM) as shown in Figure 2(E). Thus the inhibition curves of the compounds were obtained using an ATP concentration of 50 μM, and the IC_{50} as well as the resulting inhibition constant K_i could be calculated thanks to the Cheng–Prusoff relationship (eqn 3):

$$K_i = \frac{IC_{50}}{1 + \frac{[S]}{K_m}} \quad (3)$$

with $[ATP]/K_m = 1$ [45].

Experimental inhibition

All compounds were initially tested at a 50 μM concentration. When no significant variation of the reaction rates were measured (i.e. approximately 30 %), we considered the compounds as inactive.

Akt1/2 inhibitor inhibited Pontin ATPase activity with an IC_{50} of 24 μM (Figure 3A). This compound was reported to inhibit Akt1 preferentially (IC_{50} of 58 nM) with also a good potency against Akt2 (IC_{50} of 210 nM) and less against Akt3 (IC_{50} of 2.1 μM).

A non-competitive specific inhibitor of PTP1B presented an IC_{50} of 15 μM (Figure 3B), compared with 4 μM for its primary target.

Rottlerin inhibited Pontin activity with an IC_{50} of 10 μM (Figure 3C). This molecule was also reported to be a reversible inhibitor of the PKC family, although this has been questioned and it may also inhibit several MAPK family members [46]. Using the Cheng–Prusoff equation (eqn 3 [45]), the K_i values for these three molecules were determined and found to be 12.1, 7.5 and 5.1 μM respectively.

From the 15 compounds prioritized in the Prestwick Chemical Library®, only Pranlukast, a potent and specific competitive antagonist of the cysteinyl leukotriene 1 receptor, inhibited the ATPase reaction with an IC_{50} of 13 μM (Figure 3D), thus with a K_i of 6.5 μM.

The chemical structures of these compounds are shown in Figure 4.

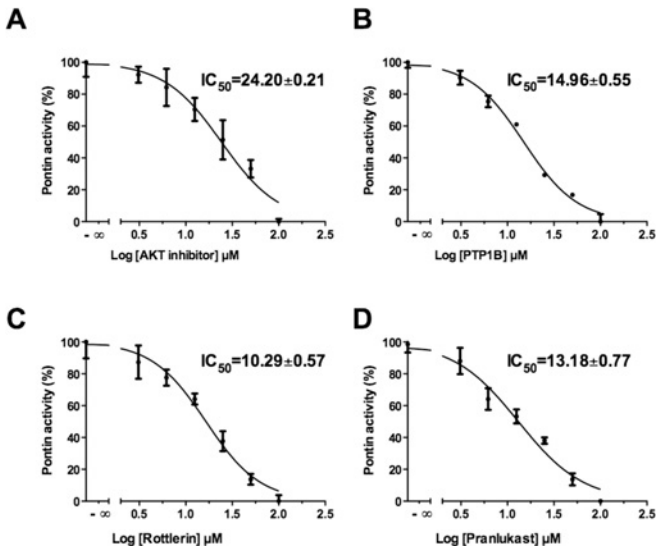

Figure 3 Identification of four inhibitors

Determination of the IC_{50} of the Akt1/2 inhibitor (**A**), the PTP1B inhibitor (**B**), Rottlerin (**C**) and Pranlukast (**D**) with 50 μM ATP and 4 μM Pontin. Results are means $\pm$ S.D. for four experiments. Some error bars cannot be seen because they were too small.

Binding pose analysis

The observation of the active-site topology led to the distinction of two spaces. The flattest part of the cavity was occupied by ADP and ATP, whereas the other side, which includes all residues from the second subunit, was left empty. The best docking poses for all active compounds shared common features with ADP and ATP (Figure 5).

Out of the 17 residues involved in the binding mode of ADP, ten were also implicated in the binding of all inhibitors. The number of residues common to the binding mode of ADP and to the ligands respectively ranged from 11 for Rottlerin, to 13 for Pranlukast and 14 for Akt and PTP1B inhibitors. Furthermore, various residues from the Walker A domain (residues 70–79) were involved in the binding mode of all ligands as well as ADP and ATP, with at least four different residues out of ten in close proximity to the ligands. As for the Walker B domain (residues 302–305), all inhibitors and ATP interacted with Asp^{302} only, whereas ADP did not make contact with it at all. This residue is crucial for the hydrolysis of ATP, as shown by the lack of ATPase activity for the D302N mutant [3].

In all cases, an aromatic cycle lay in a position close to that of the adenine. Furthermore, Pranlukast and the PTP1B inhibitor presented a hydrogen-bond acceptor group superimposed on the γ-phosphate of ATP, and created hydrogen-bonding with Gly^{73} similar to both ATP and ADP. In contrast, the pose of the Akt1/2 inhibitor prevented all hydrogen-bonding with this side of the cavity. Rottlerin was the only ligand to form a hydrogen bond with Arg^{404} from sensor 2, as in the case of ATP.

As opposed to ADP or ATP, all compounds created interactions with the second area of the cavity. This included hydrophobic contacts with the second subunit, through Asp^{353} for Rottlerin, as well as Asp^{356} for all ligands. In addition, Pranlukast and the PTP1B inhibitor made electrostatic interactions with the arginine 'finger', i.e. Arg^{357} from the second subunit. The latter even accepted two hydrogen bonds between its sulfonamide and the guanidine group from the arginine finger.

A flexible docking was also conducted on the dimer, meaning that the rotations on the side chains of the residues located in a sphere of 5 Å around the centre of mass of ADP were authorized during docking. This method aims to render the rearrangements induced by the binding of a ligand into the structure of the active site (induced fit), but the major drawback is the calculation time, which increases dramatically with the number of torsions allowed. In the model, the active site was completely buried and highly constrained. The authorized movements on the side chains were thus very limited. As expected, we have observed no noticeable modifications in the results obtained or in the poses compared with those obtained with the non-flexible dimer.

Type of enzyme inhibition

The kind of inhibition presented by these compounds was determined by measuring the rates of ATP hydrolysis with the Malachite Green assay, using five concentrations of ATP, ranging from the K_m (50 μM) to 1 mM, together with increasing concentrations of inhibitors.

The double-reciprocal plots (Figure 6) showed that Rottlerin was the only ligand that inhibited the ATPase activity competitively. In the experiments using Pranlukast and the PTP1B inhibitor, both the V_{max} and the K_m for ATP hydrolysis varied upon addition of the inhibitors, revealing a mixed or uncompetitive inhibition. The analysis of the results obtained with the Akt1/2 inhibitor revealed a more surprising inhibition profile since the double-reciprocal plots indicated that the $-1/K_m$ value was identical with the one measured for ATP, proving that the inhibitor did not compete with the ATP-binding site.

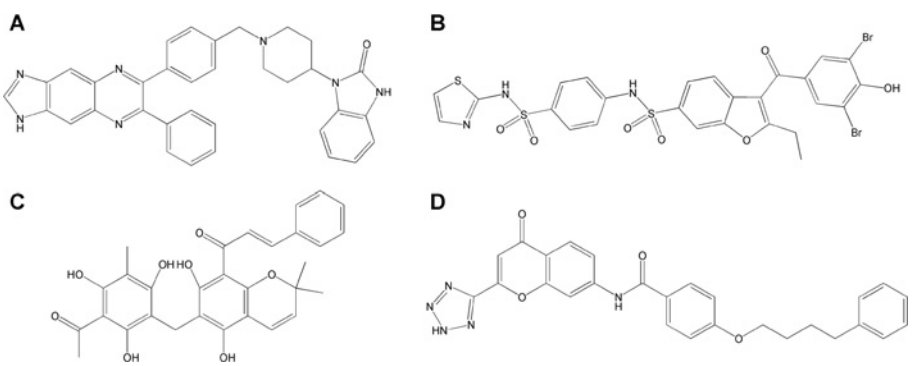

Figure 4 Chemical structures of the four active compounds

(**A**) Akt1/2 inhibitor. (**B**) PTP1B inhibitor. (**C**) Rottlerin. (**D**) Pranlukast.

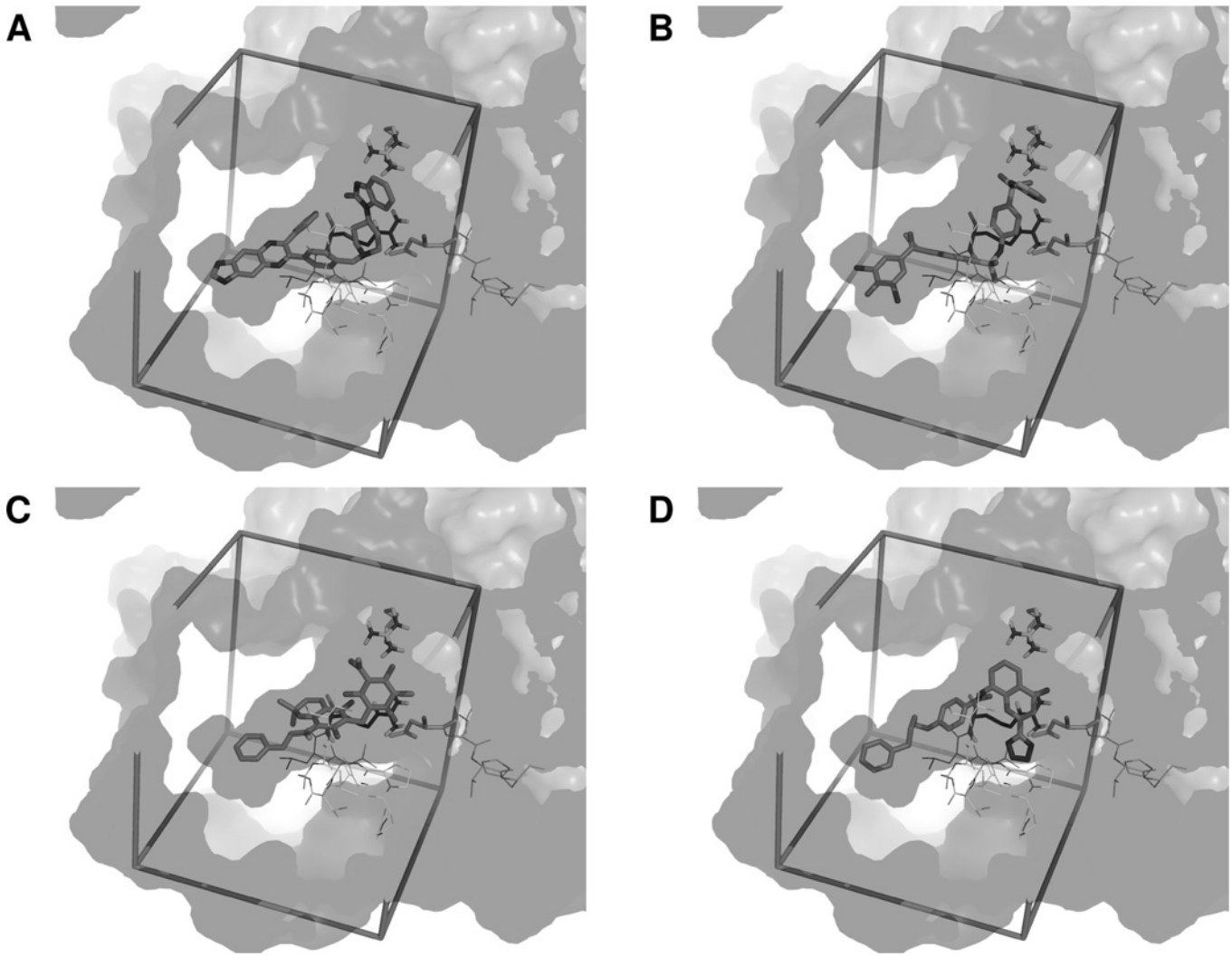

Figure 5 Docking poses in the dimer of Pontin

(**A**) The best docking pose for the Akt1/2 inhibitor is shown as sticks. The active site is represented as transparency with surfaces of both subunits of Pontin shown in different shades of grey. Important domains from the ATP-binding site are shown as lines with essential residues as sticks. From the first subunit, the Walker A domain is in front of the ligands, the Walker B domain is at the right side of the image, with Asp^{302} highlighted, and the sensor 2 is at the back of the cavity, with Arg^{404} highlighted. From the second subunit, the arginine finger (Arg^{357}) is shown as sticks. The search space box is represented in sticks. (**B**–**D**) Similar representation of the PTP1B inhibitor (**B**), Rottlerin (**C**) and Pranlukast (**D**).

The compounds tested experimentally had been selected via structure-based virtual screening. According to the literature, the docking experiments were conducted by targeting the ATP-binding site [1,19,23,24] and we therefore expected the inhibitors that were identified to bind competitively to the ATP-binding site of Pontin. Yet, among four inhibitors, only Rottlerin appeared to be competitive. Pranlukast and the PTP1B inhibitor presented a mixed or uncompetitive profile and, in the case of the Akt inhibitor, the double-reciprocal plot indicated a non-competitive inhibitor.

In order to explore other potential binding modes, additional docking experiments were conducted on the monomer of Pontin, in the presence or in the absence of ATP and ADP, considering a search space that encompassed the whole protein (blind docking). In the case of a tandem dimer docking, the search box contained only the binding site of crystallized ADP, which was completely buried since the second monomer was closing the cavity, contributing to the shape of the active site. This subunit, even if it did not create interactions with the compounds, constrained them into a closed area, playing a key role in the ligand-binding modes. In contrast, in the case of the blind docking on the monomer, the ligands had the freedom not only to explore the surface surrounding the cavity that was covered up by the second subunit in the dimer, but also to bind everywhere on the surface of whole protein.

In the case of the Akt1/2 inhibitor, similar results were obtained either using Pontin alone or in complex with ADP and ATP. Except for a few poses halfway inside the active site when Pontin was used alone, or situated at the entrance of the active site when ATP was present, almost all of the poses observed were located in a groove at the junction between domain I and domain II of the protein (Figure 7A). These poses were too far from the active site to interfere directly with the binding of ATP, but they could be interacting with the nucleotide-binding site. Actually, domain II is the seat of the DNA-binding site, and since we have shown that the presence of DNA considerably influenced the reaction rate, it is possible that the Akt1/2 inhibitor interferes with this feature.

As for Pranlukast, the blind docking has shown that when ATP was complexed with Pontin, a binding mode located at the entrance of the cavity was clearly favoured (Figure 7B). This pose could prevent ATP from being hydrolysed and does not

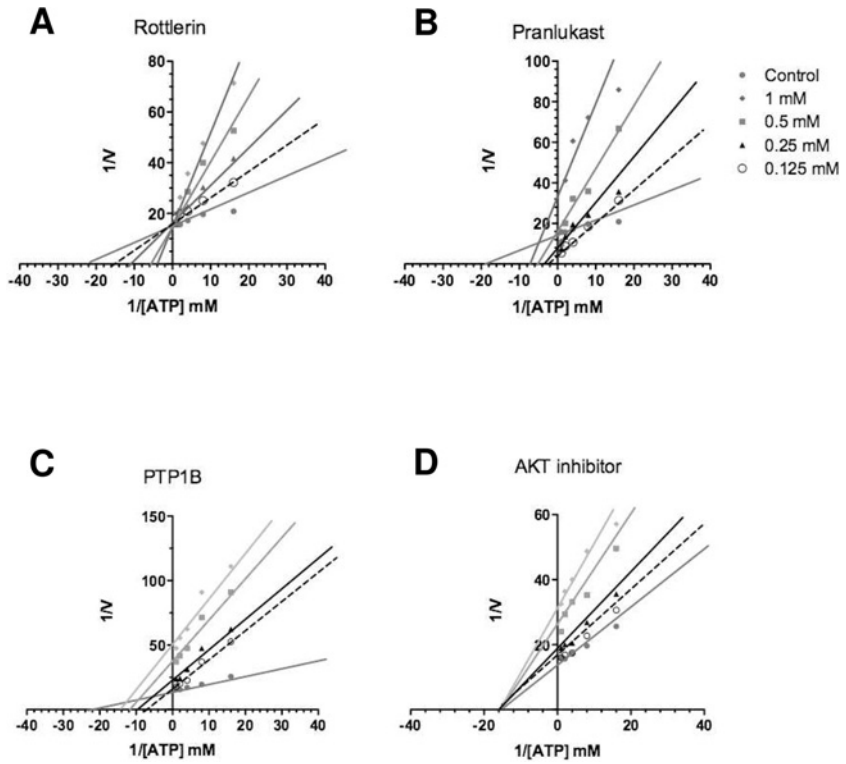

Figure 6 Types of enzyme inhibition

(**A**) Double-reciprocal plots (Lineweaver–Burk plots) of the reaction rates with ATP alone, and increasing concentrations of Rottlerin. When no variation of 1/[ATP] is observed, the inhibitor is non-competitive and does not modify the binding of ATP. In contrast, when no variation of $1/V_{max}$ is observed, the ligand is competitive and disrupts ATP binding to the protein. (**B**–**D**) Similar plots for Pranlukast (**B**), PTP1B inhibitor (**C**) and Akt1/2 inhibitor (**D**). Results are means for two independent experiments performed four times.

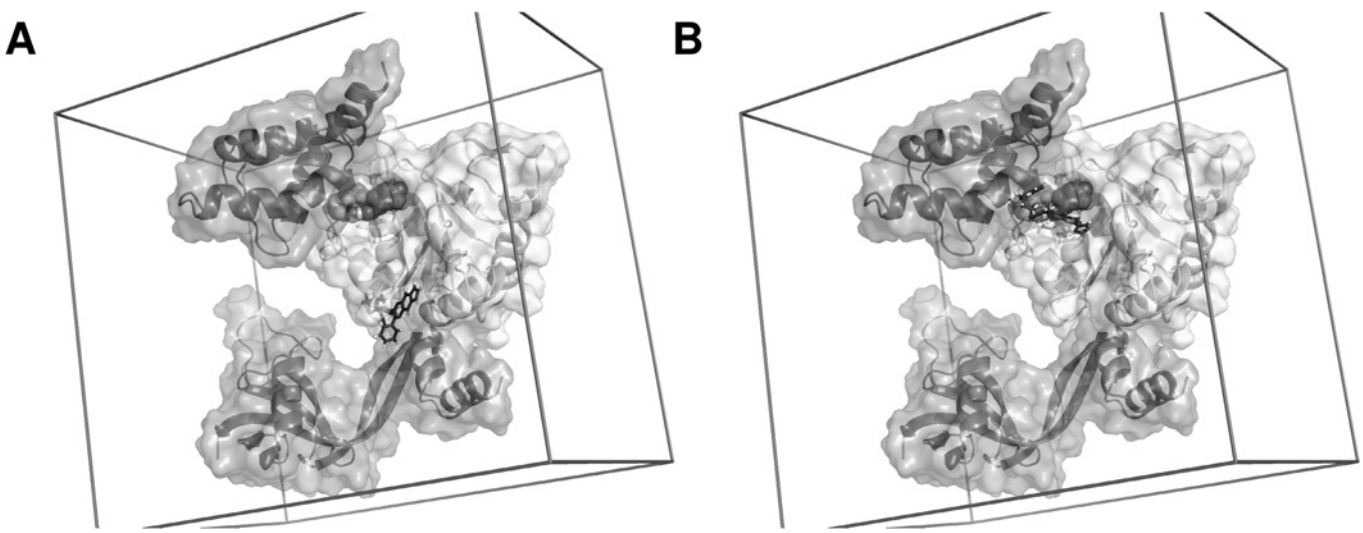

Figure 7 Docking poses obtained via blind docking

(**A**) The best docking pose for the Akt1/2 inhibitor is shown as sticks. The monomer of Pontin is represented as transparency and cartoons, with domains I, II and III coloured different shades of grey. The inhibitor lies in a groove between domain I and domain II, in close proximity to the DNA-binding site. (**B**) Similar representation for Pranlukast. The inhibitor is located at the entrance of the catalytic site.

leave sufficient space for ADP to get out. It is also incompatible with the existence of a tandem dimer similar to that observed in crystallography [3], as Pranlukast would create clashes with several residues from the second subunit. In contrast, no clear pose preference was observed when Pontin was complexed with ADP, and the best poses obtained with Pontin alone were located halfway inside the active site, which was contradictory to the experimental data. These results are consistent with the hypothesis of an uncompetitive inhibition, which implies that the enzyme is complexed by its substrate before the binding of the inhibitor. The binding of ATP would thus enable Pranlukast to bind to the protein and to inhibit its enzymatic activity.

The blind docking of the PTP1B inhibitor did not reveal such a clear-cut profile. The complexation of ATP did slightly favour the pose at the entrance of the cavity as in the case of Pranlukast, but numerous other poses were observed as well, and it was hard to define which pose was the most likely to be observed.

Taken together, these experiments would warrant further structural and biochemical studies due to the complexity of Pontin. The competitive inhibition observed with Rottlerin indicated a pure competition with the ATP-binding site which confirmed the *in silico* antagonists selection. Nonetheless, the mixed or uncompetitive inhibition measured with the PTP1B inhibitor and Pranlukast, and the non-competitive nature of the Akt inhibitor, suggest indirect interferences with the ATPase activity of Pontin, either by blocking the hydrolysis of ATP or the exit of ADP, or through interactions with the DNA-binding site. Therefore the modulation of the hydrolysis shown upon addition of DNA may be an important parameter in these processes. Actually, as shown by Mezard et al. [2] and Rottbauer et al. [44], DNA-binding and ATPase activities are tightly coupled. Moreover, the catalytic site is formed by two subunits and we can assume that the arginine finger may indirectly modulate the catalytic activity upon inhibitor binding [47]. A similar inference may be suggested by the observations of Zhang and Wigley [48] and Moffitt et al. [49], pointing to intersubunit interactions.

Effects of the inhibitors on proliferation of cultured cell lines

The hepatic tumour cell lines HuH7 and Hep3B were grown in the presence of these compounds for 4 days. As can be seen in Figure 8, Rottlerin had a strong anti-proliferative effect on both cell lines. It was toxic at concentrations higher than 5 μM for HuH7 and 1 μM for Hep3B, as was evident from cell numbers falling below the day 0 values. The Akt inhibitor behaved similarly, although it was toxic only at higher concentrations. Pranlukast was not toxic in the concentration range tested, and decreased cell proliferation of both cell lines dose-dependently. Calculated IC_{50} values in HuH7 and Hep3B cells were respectively 0.57 and 0.25 μM for Rottlerin, 4.0 and 3.5 μM for Akt1/2 inhibitor, and 63.7 and 34.3 μM for Pranlukast. Finally, the PTP1B inhibitor did not show any growth inhibition or cytotoxicity at concentrations up to 100 μM.

Altogether, three out of four molecules reduced cell numbers as seen with Pontin silencing [20], suggesting that they may indeed target Pontin within cells. Because of their cognate targets, it was expected that Rottlerin and the Akt inhibitor would have such an effect. Since these molecules are likely to act at the same time on those targets and on Pontin, it is difficult to strictly compare their *in vitro* and *in vivo* IC_{50} values and we can thus only conclude that their effects are compatible with an effect on Pontin. PTP1B inhibition can lead either to increased or reduced cell proliferation, depending on the context [50]. In our hands, the PTP1B antagonist had no effect on the growth of the hepatocellular carcinoma cell lines tested. It may be that access of the inhibitor to Pontin is hampered *in vivo*, either because of internalization or solubility issues, or because the *in vivo* conformation of the target prevents the inhibitor from accessing the catalytic centre. Finally, Pranlukast, an antagonist of the leukotriene receptor, reduced cell proliferation with a similar potency as for Pontin ATPase activity inhibition. This is of special interest since, in contrast with the other three molecules for which primary targets are nucleotide-using enzymes, Pranlukast is a competitive antagonist of a non-nucleotide molecule believed to act outside the plasma membrane.

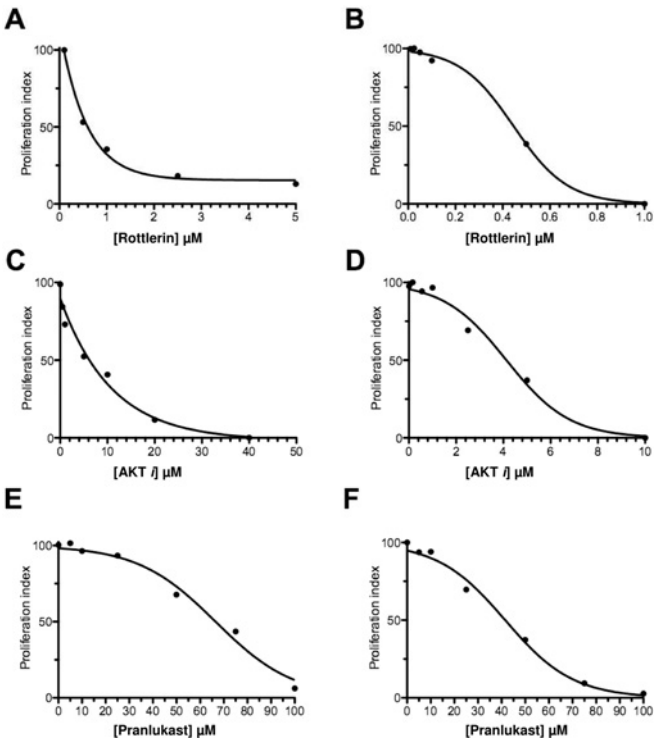

Figure 8 Cell proliferation assays

Effects of Rottlerin (**A** and **B**), Akt inhibitor (**C** and **D**) and Pranlukast (**E** and **F**) on the growth of HuH7 (**A**, **C** and **E**) and Hep3B (**B**, **D** and **F**) hepatocarcinoma cell lines. Cells were grown in the presence of various concentrations of the inhibitors (indicated in μM). Cell numbers were estimated 4 days later using the MTS assay, and the growth index was calculated as described in the Experimental section. Results are means for two independent experiments performed with five replicates each.

Conclusions

Using *in silico* and *in vitro* complementary approaches, the present paper discloses the first identification of inhibitors of the ATPase activity of Pontin, an activity required for several biological functions [9].

The first step involved structural modelling of the ATP-binding centre, and virtual screening of approximately 2200 commercial compounds using Vina. Thorough rescoring of the poses with Xscore and DrugScore, using 29 decoys as a negative calibration set, allowed the selection of efficient scoring functions for this system. Various consensuses using these functions were compared, and the intersection of Vina, SURF score from DrugScore and HPscore from Xscore scores appeared to provide the best results. With regard to these results, this consensus was used to prioritize 25 compounds for experimental testing. This virtual screening strategy proved efficient, since post-experimental analysis of the results indicated that the consensus scoring used to discriminate the compounds was the only one that allowed the selection of the four active molecules. Similarly, none of the single functions had detected all four ligands in their top-scoring lists.

The enzymatic testing of chemicals selected by docking with a Malachite Green assay was made possible because of improvements in the procedure, and in particular the addition of polynucleotides that increased the reaction rates severalfold. Four ligands displayed an inhibition constant in the micromolar range. The colorimetric assay described in the present paper could also be used for high-throughput screenings, because of its sensitivity

and rapidity compared with the current time-consuming use of radiolabelled ATP.

Finally, three of the four compounds tested reduced cell growth at concentrations close to those inhibiting the ATPase activity of Pontin *in vitro*. Whether their anti-proliferative action is due to Pontin antagonism will require further study.

AUTHOR CONTRIBUTION

Judith Elkaim designed, performed and analysed the virtual screening experiments. Michel Castroviejo provided invaluable help in protein purification. Driss Bennani designed and wrote specific scripts for the virtual screening analysis. Said Taouji adapted and performed the robotized biochemical screening, analysed the results and prepared the corresponding Figures. Nathalie Allain and Patrick Lestienne performed the protein purification, and participated in the biochemical testing, analysis and Figure preparation. Michel Laguerre prepared the three-dimensional structure of Pontin and designed the virtual screening experiments. Patrick Lestienne designed the overall biochemical experiment and realized the enzymatic assay. Jean Dessolin designed the virtual screening experiments and analysed the results. Judith Elkaim, Said Taouji, Michel Laguerre, Jean Rosenbaum, Patrick Lestienne and Jean Dessolin discussed the data. Judith Elkaim, Jean Rosenbaum, Patrick Lestienne and Jean Dessolin wrote the paper.

ACKNOWLEDGEMENTS

We thank the French Chimiothèque Nationale for initial studies. We gratefully acknowledge Dr I.R. Tsaneva for the gift of the plasmid and for helpful and friendly discussion. We express our warmest thanks to Dr S.-H. Wang (Graduate Institute of Pharmaceutical Chemistry, China Medical University, Taiwan) for providing DBfilter and Dr M.L. Jung from Prestwick.

FUNDING

This project was supported by grants from Ligue Nationale Contre le Cancer, Association pour la Recherche sur le Cancer and Institut National du Cancer [grant number PLBIO10-155]. We thank the MENRT (Ministere de l'Education Nationale de la Recherche et de Technologie), CNRS (Centre National de la Recherche Scientifique) and INSERM (Institut National de la Santé et de la Recherche Médicale) for their support.

REFERENCES

1 Jonsson, Z. O., Dhar, S. K., Narlikar, G. J., Auty, R., Wagle, N., Pellman, D., Pratt, R. E., Kingston, R. and Dutta, A. (2001) Rvb1p and Rvb2p are essential components of a chromatin remodeling complex that regulates transcription of over 5 % of yeast genes. J. Biol. Chem. **276**, 16279–16288

2 Mezard, C., Davies, A. A., Stasiak, A. and West, S. C. (1997) Biochemical properties of the RuvB^{D113N}: a mutation in helicase motif II of the RuvB hexamer affects DNA binding and ATPase activities. J. Mol. Biol. **271**, 704–717

3 Matias, P. M., Gorynia, S., Donner, P. and Carrondo, M. A. (2006) Crystal structure of the human AAA+ protein RuvBL1. J. Biol. Chem. **281**, 38918–38929

4 Ammelburg, M., Frickey, T. and Lupas, A. N. (2006) Classification of AAA+ proteins. J. Struct. Biol. **156**, 2–11

5 Gribun, A., Cheung, K. L., Huen, J., Ortega, J. and Houry, W. A. (2008) Yeast Rvb1 and Rvb2 are ATP-dependent DNA helicases that form a heterohexameric complex. J. Mol. Biol. **376**, 1320–1333

6 Puri, T., Wendler, P., Sigala, B., Saibil, H. and Tsaneva, I. R. (2007) Dodecameric structure and ATPase activity of the human TIP48/TIP49 complex. J. Mol. Biol. **366**, 179–192

7 Torreira, E., Jha, S., Lopez-Blanco, J. R., Arias-Palomo, E., Chacon, P., Canas, C., Ayora, S., Dutta, A. and Llorca, O. (2008) Architecture of the pontin/reptin complex, essential in the assembly of several macromolecular complexes. Structure **16**, 1511–1520

8 Gorynia, S., Bandeiras, T. M., Pinho, F. G., McVey, C. E., Vonrhein, C., Round, A., Svergun, D. I., Donner, P., Matias, P. M. and Carrondo, M. A. (2011) Structural and functional insights into a dodecameric molecular machine: the RuvBL1/RuvBL2 complex. J. Struct. Biol. **176**, 279–291

9 Grigoletto, A., Lestienne, P. and Rosenbaum, J. (2011) The multifaceted proteins Reptin and Pontin as major players in cancer. Biochim. Biophys. Acta **1815**, 147–157

10 Jha, S. and Dutta, A. (2009) RVB1/RVB2: running rings around molecular biology. Mol. Cell **34**, 521–533

11 Jin, J., Cai, Y., Yao, T., Gottschalk, A. J., Florens, L., Swanson, S. K., Gutierrez, J. L., Coleman, M. K., Workman, J. L., Mushegian, A. et al. (2005) A mammalian chromatin remodeling complex with similarities to the yeast INO80 complex. J. Biol. Chem. **280**, 41207–41212

12 Shen, X., Mizuguchi, G., Hamiche, A. and Wu, C. (2000) A chromatin remodelling complex involved in transcription and DNA processing. Nature **406**, 541–544

13 Jha, S., Shibata, E. and Dutta, A. (2008) Human Rvb1/Tip49 is required for the histone acetyltransferase activity of Tip60/NuA4 and for the downregulation of phosphorylation on H2AX after DNA damage. Mol. Cell. Biol. **28**, 2690–2700

14 Gallant, P. (2007) Control of transcription by Pontin and Reptin. Trends Cell. Biol. **17**, 187–192

15 Bauer, A., Chauvet, S., Huber, O., Usseglio, F., Rothbacher, U., Aragnol, D., Kemler, R. and Pradel, J. (2000) Pontin52 and reptin52 function as antagonistic regulators of β-catenin signalling activity. EMBO J. **19**, 6121–6130

16 Wood, M. A., McMahon, S. B. and Cole, M. D. (2000) An ATPase/helicase complex is an essential cofactor for oncogenic transformation by c-Myc. Mol. Cell **5**, 321–330

17 Watkins, N. J., Dickmanns, A. and Luhrmann, R. (2002) Conserved stem II of the box C/D motif is essential for nucleolar localization and is required, along with the 15.5K protein, for the hierarchical assembly of the box C/D snoRNP. Mol. Cell. Biol. **22**, 8342–8352

18 Boulon, S., Marmier-Gourrier, N., Pradet-Balade, B., Wurth, L., Verheggen, C., Jady, B. E., Rothe, B., Pescia, C., Robert, M. C., Kiss, T. et al. (2008) The Hsp90 chaperone controls the biogenesis of L7Ae RNPs through conserved machinery. J. Cell Biol. **180**, 579–595

19 Venteicher, A. S., Meng, Z., Mason, P. J., Veenstra, T. D. and Artandi, S. E. (2008) Identification of ATPases pontin and reptin as telomerase components essential for holoenzyme assembly. Cell **132**, 945–957

20 Haurie, V., Menard, L., Nicou, A., Touriol, C., Metzler, P., Fernandez, J., Taras, D., Lestienne, P., Balabaud, C., Bioulac-Sage, P. et al. (2009) Adenosine triphosphatase pontin is overexpressed in hepatocellular carcinoma and coregulated with reptin through a new posttranslational mechanism. Hepatology **50**, 1871–1883

21 Rousseau, B., Menard, L., Haurie, V., Taras, D., Blanc, J., Moreau-Gaudry, F., Metzler, P., Hugues, M., Boyault, S., Lemiere, S. et al. (2007) Overexpression and role of the ATPase and putative DNA helicase RuvB-like 2 in human hepatocellular carcinoma. Hepatology **46**, 1108–1118

22 Menard, L., Taras, D., Grigoletto, A., Haurie, V., Nicou, A., Dugot-Senant, N., Costet, P., Rousseau, B. and Rosenbaum, J. (2010) *In vivo* silencing of Reptin blocks the progression of human hepatocellular carcinoma in xenografts and is associated with replicative senescence. J. Hepatol. **52**, 681–689

23 King, T. H., Decatur, W. A., Bertrand, E., Maxwell, E. S. and Fournier, M. J. (2001) A well-connected and conserved nucleoplasmic helicase is required for production of box C/D and H/ACA snoRNAs and localization of snoRNP proteins. Mol. Cell. Biol. **21**, 7731–7746

24 Lim, C. R., Kimata, Y., Ohdate, H., Kokubo, T., Kikuchi, N., Horigome, T. and Kohno, K. (2000) The *Saccharomyces cerevisiae* RuvB-like protein, Tih2p, is required for cell cycle progression and RNA polymerase II-directed transcription. J. Biol. Chem. **275**, 22409–22417

25 Feng, Y., Lee, N. and Fearon, E. R. (2003) TIP49 regulates β-catenin-mediated neoplastic transformation and T-cell factor target gene induction via effects on chromatin remodeling. Cancer Res. **63**, 8726–8734

26 Dugan, K. A., Wood, M. A. and Cole, M. D. (2002) TIP49, but not TRRAP, modulates c-Myc and E2F1 dependent apoptosis. Oncogene **21**, 5835–5843

27 Qiu, X. B., Lin, Y. L., Thome, K. C., Pian, P., Schlegel, B. P., Weremowicz, S., Parvin, J. D. and Dutta, A. (1998) An eukaryotic RuvB-like protein (RUVBL1) essential for growth. J. Biol. Chem. **273**, 27786–27793

28 Ikura, T., Ogryzko, V. V., Grigoriev, M., Groisman, R., Wang, J., Horikoshi, M., Scully, R., Qin, J. and Nakatani, Y. (2000) Involvement of the TIP60 histone acetylase complex in DNA repair and apoptosis. Cell **102**, 463–473

29 Choi, J., Heo, K. and An, W. (2009) Cooperative action of TIP48 and TIP49 in H2A.Z exchange catalyzed by acetylation of nucleosomal H2A. Nucleic Acids Res. **37**, 5993–6007

30 Trott, O. and Olson, A. J. (2010) AutoDock Vina: improving the speed and accuracy of docking with a new scoring function, efficient optimization, and multithreading. J. Comput. Chem. **31**, 455–461

31 Velec, H. F. G., Gohlke, H. and Klebe, G. (2005) DrugScore^{CSD}: knowledge-based scoring function derived from small molecule crystal data with superior recognition rate of near native ligand poses and better affinity prediction. J. Med. Chem. **48**, 6296–6303

32 Gohlke, H., Hendlich, M. and Klebe, G. (2000) Knowledge-based scoring function to predict protein–ligand interactions. J. Mol. Biol. **295**, 337–356

33 Wang, R., Laib, L. and Wang, S. (2002) Further development and validation of empirical scoring functions for structure-based binding affinity prediction. J. Comput. Aided Mol. Des. **16**, 11–26

34 O'Boyle, N. M., Banck, M., James, C. A., Morley, C., Vandermeersch, T. and Hutchison, G. R. (2011) Open Babel: an open chemical toolbox. J. Cheminform. **3**, 33

35 Sanner, M. F. (1999) Python: a programming language for software integration and development. J. Mol. Graphics Modell. **17**, 57–61
36 Morris, G. M., Goodsell, D. S., Halliday, R. S., Huey, R., Hart, W. E., Belew, R. K. and Olson, A. J. (1998) Automated docking using a Lamarckian genetic algorithm and an empirical binding free energy function. J. Comput. Chem. **19**, 1639–1662
37 Chang, M. W., Ayeni, C., Breuer, S. and Torbett, B. E. (2010) Virtual screening for HIV protease inhibitors: a comparison of AutoDock 4 and Vina. PLoS ONE **5**, e11955
38 Guha, R., Howard, M. T., Hutchison, G. R., Murray-Rust, P., Rzepa, H., Steinbeck, C., Wegner, J. K. and Willighagen, E. (2006) The Blue Obelisk: interoperability in chemical informatics. J. Chem. Inf. Model. **46**, 991–998
39 Zhang, J. H., Chung, T. D. and Oldenburg, K. R. (1999) A simple statistical parameter for use in evaluation and validation of high throughput screening assays. J. Biomol. Screen. **4**, 67–73
40 Charifson, P. S., Corkery, J. J., Murcko, M. A. and Walters, W. P. (1999) Consensus scoring: a method for obtaining improved hit rates from docking databases of three-dimensional structures into proteins. J. Med. Chem. **42**, 5100–5109
41 Wang, R. and Wang, S. (2001) How does consensus scoring work for virtual library screening? An idealized computer experiment. J. Chem. Inf. Comput. Sci. **41**, 1422–1426
42 Kanemaki, M., Kurokawa, Y., Matsu-ura, T., Makino, Y., Masani, A., Okazaki, K., Morishita, T. and Tamura, T. A. (1999) TIP49b, a new RuvB-like DNA helicase, is included in a complex together with another RuvB-like DNA helicase, TIP49a. J. Biol. Chem. **274**, 22437–22444
43 Makino, Y., Kanemaki, M., Kurokawa, Y., Koji, T. and Tamura, T.-A. (1999) A rat Ruv-B like Protein, TIP49a, is a germ cell-enriched novel DNA helicase. J. Biol. Chem. **274**, 15329–15335
44 Rottbauer, W., Saurin, A. J., Lickert, H., Shen, X., Burns, C. G., Wo, Z. G., Kemler, R., Kingston, R., Wu, C. and Fishman, M. (2002) Reptin and pontin antagonistically regulate heart growth in zebrafish embryos. Cell **111**, 661–672
45 Cheng, Y. and Prusoff, W. H. (1973) Relationship between inhibition constant (K_i) and the concentration of inhibitor which causes 50 per cent inhibition (I_{50}) of an enzymatic reaction. Biochem. Pharmacol. **22**, 3099–3108
46 Soltoff, S. P. (2007) Rottlerin: an inappropriate and ineffective inhibitor of PKCδ. Trends Pharmacol. Sci. **28**, 453–458
47 Hishida, T., Han, Y. W., Fujimoto, S., Iwasaki, H. and Shinagawa, H. (2004) Direct evidence that a conserved arginine in RuvB AAA+ ATPase acts as an allosteric effector for the ATPase activity of the adjacent subunit in hexamer. Proc. Natl. Acad. Sci. U.S.A. **101**, 9573–9577
48 Zhang, X. and Wigley, D. B. (2008) The "glutamate switch" provides a link, between ATPase activity and ligand binding in AAA + proteins. Nat. Struct. Mol. Biol. **11**, 1223–1227
49 Moffitt, J. R., Chemila, Y. R., Aathavan, K., Grimes, S., Jardine, P. J., Anderson, D. L. and Bustamante, C. (2009) Intersubunit coordination in a homomeric ring ATPase. Nature **457**, 446–450
50 Lessard, L., Stuible, M. and Tremblay, M. (2010) The two faces of PTP1B in cancer. Biochim. Biophys. Acta **1804**, 613–619

Received 5 October 2011/23 January 2012; accepted 24 January 2012
Published as BJ Immediate Publication 24 January 2012, doi:10.1042/BJ20111779

Biochem. J. (2012) **443**, 549–559 (Printed in Great Britain) doi:10.1042/BJ20111779

online data

SUPPLEMENTARY ONLINE DATA

First identification of small-molecule inhibitors of Pontin by combining virtual screening and enzymatic assay

Judith ELKAIM*, Michel CASTROVIEJO†, Driss BENNANI*, Said TAOUJI‡, Nathalie ALLAIN‡, Michel LAGUERRE*, Jean ROSENBAUM‡, Jean DESSOLIN*[1] and Patrick LESTIENNE‡[1]

*Molecular Modeling Group, IECB-CNRS-Université de Bordeaux, UMR 5248, 2 rue R. Escarpit, F-33607 Pessac, France, †Platform Protein Expression and Purification, CNRS, UMR 5234, 146 rue L. Saignat, F-33076 Bordeaux Cedex, France, and ‡Physiopathologie du Cancer du Foie, INSERM U1053-Université de Bordeaux, 146 rue L. Saignat, F-33076 Bordeaux Cedex, France

VIRTUAL SCREENING

Individual scoring functions

DrugScore provides three scoring functions, i.e. PAIR, SURF and PAIRSURF, and two alternative versions of DrugScore are available: DrugScore^{CSD} [1] and DrugScore^{PDB} [2]. For both versions, SURF score is identical and PAIRSURF score is the sum of PAIR and SURF score. Consequently, five distinct functions are available from DrugScore, that will be noted PAIR_csd, PAIRSURF_csd, PAIR_pdb, PAIRSURF_pdb and SURF. Xscore [3] offers four scoring functions that are HPscore, HMscore, HSscore and AVEscore, with the last being the average of the first three.

At first, all scoring functions were evaluated individually by comparing the number of decoys ranked in the best 15 % (139 compounds) of the training set (Table S1).

All dockings were performed with Vina [4], meaning that its scoring function was used during the process of poses generation. Therefore the correctness of this function was a key factor for the accuracy of the whole experiment. Out of the 929 compounds present in the training set, two decoys appeared in the top 15 % with the scoring function inherent to Vina.

The functions from DrugScore^{CSD} clearly failed to discriminate the decoys. With PAIRSURF_csd and PAIR_csd, five decoys were found in the top 15 %. The PDB version of DrugScore performed better, with both PAIRSURF_pdb and PAIR_pdb ranking only one decoy in the best 15 %. Similarly, SURF ranked only decoy in the top 15 %.

The best results were obtained with the functions from Xscore. AVEscore and HPscore both ranked only one decoy in the best 15 %, and HSscore and HMscore were very efficient at excluding the decoys from the top, since no decoy was observed in the best 15 %.

Consensus scoring

From now on, a consensus will be noted as follows: 'Function1/Function2 X', with X being the percentage of base considered for each function. To discriminate the combinations that were able to exclude the decoys from the top-scoring compounds, the consensuses were first carried out by keeping up to 30 % of the base for each function, i.e. 279 compounds, and then progressively reducing the percentage of base considered. Using the *Consensus Scoring* protocol from Discovery Studio 2.1, the numerous combinations available with the ten scoring functions were explored. However, the combinations of different scoring functions coming from the same program were not considered since the functions are not independent [5].

The combinations of SURF with all functions from Xscore were explored first, since those functions were the best at discriminating between the decoys individually. The consensuses obtained showed that the results given by those functions were highly correlated, in particular in the consensus HPscore/SURF 30, where up to 242 compounds out of 279 in the best 30 % were common to both top lists, including only one decoy. Similar results were observed with HSscore/SURF 30 with 217 common compounds, among which one was a decoy. HMscore/SURF 30 and AVEscore/SURF 30 gave poorer results, with 204 and 220 molecules respectively shared by both functions, including two decoys. Yet, none of these consensuses was able to completely exclude the decoys.

The consensuses made with Vina displayed a much lower number of common ligands. In the consensus Vina/SURF 30, 127 molecules were shared by both functions, but two of these were decoys. As for Vina/HMscore 30 and Vina/AVEscore 30, they provided 128 and 121 shared compounds respectively, including one decoy. Vina/HSscore 30 and Vina/HPscore 30 did best at eliminating the decoys from the top since 119 and 125 compounds respectively responded to both individual functions, with no decoys.

Using three functions, the consensuses Vina/HSscore/SURF 30 and Vina/HPscore/SURF 30 gave very similar results, with 100 and 108 compounds respectively responding to the three functions, with no decoys.

Table S1 Decoy discrimination, single functions

Number and ranks (in parentheses) of the decoys found in the top 15 % of the training set (Calbiochem database + decoys).

Functions	Decoys
Vina	2 (51, 109)
PAIR_csd	5 (21, 32, 57, 58, 81)
PAIRSURF_csd	5 (30, 36, 43, 65, 104)
PAIR_pdb	1 (51)
PAIRSURF_pdb	1 (53)
SURF	1 (37)
HPscore	1 (95)
HMscore	–
HSscore	–
AVEscore	1 (83)

[1] Correspondence may be addressed to either of these authors (email j.dessolin@iecb.u-bordeaux.fr for molecular modelling aspects or patrick.lestienne@inserm.fr for biochemical aspects).

Table 2 Decoy discrimination, consensus

Number of common ligands in the consensus 30 % and number of decoys found among them (Calbiochem database + decoys).

Functions	Common	Number of decoys
HP/SURF	242	1
HM/SURF	204	2
HS/SURF	217	1
AVE/SURF	220	2
Vina/SURF	127	2
Vina/HS	119	–
Vina/HM	128	1
Vina/HP	125	–
Vina/AVE	121	1
Vina/HS/SURF	100	–
Vina/HP/SURF	108	–

REFERENCES

1 Velec, H. F. G., Gohlke, H. and Klebe, G. (2005) DrugScore^{CSD}: knowledge-based scoring function derived from small molecule crystal data with superior recognition rate of near native ligand poses and better affinity prediction. J. Med. Chem. **48**, 6296–6303

2 Gohlke, H., Hendlich, M. and Klebe, G. (2000) Knowledge-based scoring function to predict protein–ligand interactions. J. Mol. Biol. **295**, 337–356

3 Wang, R., Laib, L. and Wang, S. (2002) Further development and validation of empirical scoring functions for structure-based binding affinity prediction. J. Comput. Aided Mol. Des. **16**, 11–26

4 Trott, O. and Olson, A. J. (2010) AutoDock Vina: Improving the speed and accuracy of docking with a new scoring function, efficient optimization, and multithreading. J. Comput. Chem. **31**, 455–461

5 Wang, R. and Wang, S. (2001) How does consensus scoring work for virtual library screening? An idealized computer experiment. J. Chem. Inf. Comput. Sci. **41**, 1422–1426

Received 5 October 2011/23 January 2012; accepted 24 January 2012
Published as BJ Immediate Publication 24 January 2012, doi:10.1042/BJ20111779